CBPF-NF-023/81

A SIMPLE MODEL APPROACH TO LOCALIZED-ITINERANT MAGNETISM: APPLICATION TO RARE-EARTH INTERMETALLICS

by

Lucio Iannarela*, A.P.Guimarães, X.A. da Silva

*-Departamento de Física, Universidade Federal Rural de Rio de Janeiro, 23460, RJ, Brazil

-Centro Brasileiro de Pesquisas Físicas/CNPq
Av. Wenceslau Braz, 71 Fundos - R.J.
22290 - Rio de Janeiro - Brasil

ABSTRACT

The combined role of intraband and electron-localized moment exchange in determining the magnetic behaviour of a system composed of itinerant electrons and localized magnetic moments is investigated. Having in mind rare-earth-transition metal and rare-earth-normal metal intermetallic compounds, the critical temperature versus de Gennes factors and the temperature dependence of the magnetizations and susceptibilities of the two magnetic species are studied. Results are obtained for two cases, a) a delta-like band (narrow band limit), and b) a parabolic density of states, using the molecular field approximation both in the treatment of intraband interaction (Stoner-like description) and electron-localized spin exchange. Some comments are made on the parallel between computed and measured magnetic quantities in the systems RAl_2, RFe_2 and $R(Fe_{1-x}Al_x)_2$ ($0<x<1$ and $R\equiv$ heavy rare-earth).

1. INTRODUCTION

The magnetic behaviour of intermetallic compounds containing rare-earth metals and transition metals, or normal metals, has been increasingly studied (Taylor (1971), Buschow (1977), Kirchmayr and Poldy (1978), Burzo (1980). In particular, regularities in the critical temperatures as a function of the parameter of the rare-earth (e.g. the de Gennes factor) or as a function of the relative concentration of the components, and the temperature dependence of the magnetization and susceptibility have been measured. These results have been understood in terms of simple models that either treat the magnetic carriers (associated to the rare-earth or to the transition metal) as localized (e.g. Ilarraz and del Moral (1980)) or attribute to the conduction electrons (associated, e.g. to the 3d-4s bands in the iron series or the 5d-6s bands of the rare-earth) a more explicit role. This role is that of a vehicle of the interaction between the rare-earths (e.g. Debray and Sakurai (1974)) or as a carrier of itinerant magnetism, contributing to the total magnetic moment of the system (e.g. Gomes and Guimarães (1974)). This latter point of view is particularly interesting when the partner of the rare-earth is a transition metal.

The study of the temperature dependence of the magnetic susceptibility of the RCo_2 compounds was made by Bloch and Lemaire (1970) using the molecular field approximation: a molecular field arising from the ionic part acts on the electronic part, and vice versa. Phenomenological parameters measuring the electron - ion, electron-electron, and ion-ion interactions were determined by fitting the experimental results. Wohlfarth (1979) relates the

Curie temperatures T_c of intermetallics of heavy rare-earths containing cobalt to the position of the rare-earth in the periodic table, extending the analysis of Bloch et al. (1975) for cobalt concentrations that make the Y-Co system magnetic. It is interesting to note that the idea of a system of interacting localized and itinerant moments was originally applied to the study of transition metal magnetism (see Herring (1966) for a full discussion) although in that case the existence of localized moments is an open question, in opposition to the situation of rare-earth magnetism. The model that embodies this idea, sometimes referred to as Zener-Vonsovskii model, has been adopted by Stearns (1973) and by Sakoh and Edwards (1975), and more recently, Borgiel et al. (1980).

In the present work we have investigated, in the molecular field approximation, the relative importance of the electron-electron and electron-ion interactions on the magnetic behaviour of a system in which localized spins coexist and interact with conduction electrons; the conduction electrons also interact with each other. We have examined the following quantities: 1) electronic magnetization at T = 0; 2) critical temperatures; 3) temperature dependence of the electronic and ionic magnetizations and susceptibilities. Two cases were considered: the narrow-band limit and the wide-band limit (parabolic density of states).

The structure of the paper is as follows: in Section 2 the model Hamiltonian is presented and the parameters that describe the rare-earths and the conduction electrons are made explicit. In the molecular field approximation, equations that relate the magnetizations (ionic and electronic) and the chemical potential to the temperature and to the parameters of the model, are obtained. In Section 3, the narrow-band case is studied, and in Section 4, the case of a parabolic density of states. Finally, in Section 5, some comments are made on the connection between the present results and magnetic data for the intermetallic compounds of the heavy rare-earth metals.

2. FORMULATION OF THE PROBLEM

The model Hamiltonian is

$$\mathcal{H} = \mathcal{H}_e + \mathcal{H}_{e-i} + \mathcal{H}_{Zeeman} \tag{1}$$

where

$$\mathcal{H}_e = \sum_{ij\sigma} T_{ij}\, C^+_{i\sigma}\, C_{j\sigma} + I \sum_i n_{i\uparrow} n_{i\downarrow} \tag{2a}$$

$$\mathcal{H}_{e-i} = -(g-1)\, J_o \sum_\ell J^z_\ell\, s^z_\ell \tag{2b}$$

$$\mathcal{H}_{Zeeman} = -\mu_B\, H_o \sum_\ell (2\, s^z_\ell + g\, J^z_\ell) \tag{2c}$$

where $T_{ij} = 1/N \sum_{\tilde{k}} \varepsilon_{\tilde{k}}\, e^{-i\tilde{k}(\tilde{R}_i - \tilde{R}_j)}$, $\varepsilon_{\tilde{k}}$ is the energy of the band electron, I is the intra-band interaction, $C_{i\sigma}$ ($C^+_{i\sigma}$) is the destruction (or creation) operator at site i with spin $\sigma(\uparrow \text{or} \downarrow)$, J_o is the electron-ion exchange interaction, g is Landé's factor of the rare-earth, J^z_i and s^z_i are the projections of the angular momentum operators, respectively, for the ion and conduction electrons at site i, and H_o is the applied magnetic field.

The Hamiltonian (1) is similar to that used by Bloch et al. (1975); we have attempted to use in our formulation a set of physically significant parameters (J_o, I , etc), the meaning of which is implied in the model Hamiltonian, rather than purely phenomenological parameters (e.g. J_{RM}, J_{MM} as usual in the literature (see the review of Burzo (1980))). Although in the intermetallic compound series the heavy rare-earth moment couples antiferromagnetically to the electron band, we have taken $J_o>0$, since the individual magnetizations (electronic and ionic) depend only on $|J_o|$.

The basic magnetic quantities are the electronic magnetization and the ionic magnetization:

$$M_e = 2N_e\mu_B <s^z> \qquad (3a)$$

$$M_i = gN_i\mu_B <J^z> \qquad (3b)$$

where N_e and N_i are the number of electrons and ions in the sample.

$<s^z>$ and $<J^z>$ are computed in the molecular field approximation: the electron gas is subjected to the external magnetic field and to the effective field arising from the ionic and electronic magnetization ; conversely, the ions feel the external field and the field associated to the magnetization of the band. This self-consistent magnetization process is described by the following equations:

$$\mu_B\sum_{\underset{\sim}{k}} \left[f(\bar{\varepsilon}_{\underset{\sim}{k}\uparrow}) - f(\bar{\varepsilon}_{\underset{\sim}{k}\downarrow})\right] = M_e \qquad (4a)$$

$$\sum_{\underset{\sim}{k}} \left[f(\bar{\varepsilon}_{\underset{\sim}{k}\uparrow}) + f(\bar{\varepsilon}_{\underset{\sim}{k}\downarrow}) \right] = N_e \tag{4b}$$

$$gJN_i B_J(x) = M_i = gJN_i \zeta_i \tag{4c}$$

where

$$x = \frac{g\, J\mu_B H_i}{k_B T} \quad , \tag{5}$$

$$\bar{\varepsilon}_{\underset{\sim}{k}\sigma} = \varepsilon_{\underset{\sim}{k}} - \sigma\mu_B\, H_e \tag{6}$$

and $B_J(x)$ is the Brillouin function.

The magnetic fields acting on the electrons and on the ions are, respectively

$$H_e = H_o + \frac{1}{\mu_B} (J(g-1)J_o\zeta_i + k_B\theta'\zeta_e) \tag{7a}$$

$$H_i = H_o + \frac{1}{\mu_B} (g-1)J_o\zeta_e \tag{7b}$$

The function $f(\bar{\varepsilon}_{\underset{\sim}{k}\sigma})$ is given by

$$f(\bar{\varepsilon}_{\underset{\sim}{k}\sigma}) = \frac{1}{e^{\beta(\bar{\varepsilon}_{\underset{\sim}{k}\sigma}-\mu)}+1} \tag{8}$$

where μ is the chemical potential, $\beta = 1/k_BT$, $k_B\theta' = I/2$ is the intra-band interaction in the Stoner (1951) notation, and the normalized electronic and ionic magnetizations are given by

$$\zeta_e = \frac{M_e}{N_e\mu_B} \quad , \quad \zeta_i = \frac{M_i}{gJN_i\mu_B} \tag{9}$$

In order to investigate the influence of electron - ion and electron-electron interactions on the behaviour of the magnetic quantities, equations 4 are examined under the following conditions:

a) in the limit T=0; here, the equi-ζ_e curves are obtained in the plane $(g-1)J_o \times k_B\theta'$;

b) in the limit $T=T_c$; here, the equi-T_c curves are obtained in the same plane of a);

c) for $T \leq T_c$; in this case, the temperature dependence of the electronic and of the ionic magnetizations is obtained, for several pairs of parameters $\left[(g-1)J_o; k_B\theta'\right]$, for the same value of T_c;

d) for $T \geq T_c$; in this case, the temperature dependence of the susceptibilities (electronic and ionic) is obtained.

The analysis is done in two limits: narrow-band limit (Section 3) and wide-band limit (parabolic density of states; Section 4)

3. <u>NARROW-BAND LIMIT</u>

In this limit, $\varepsilon_{\underset{\sim}{k}} = \varepsilon_o$ for every $\underset{\sim}{k}$, and the equations 4a and 4b reduce to

$$\frac{1}{e^{\beta(\varepsilon_o-\mu_B H_e-\mu)}+1} - \frac{1}{e^{\beta(\varepsilon_o+\mu_B H_e-\mu)}+1} = \zeta_e \qquad (10a)$$

$$\frac{1}{e^{\beta(\varepsilon_o-\mu_B H_e-\mu)}+1} + \frac{1}{e^{\beta(\varepsilon_o+\mu_B H_e-\mu)}+1} = 1 \qquad (10b)$$

The physical solutions of equations (10) and (4c) are obtained from

$$\zeta_e = \tanh\left\{\frac{1}{2k_BT}\left[k_B\theta'\zeta_e + J(g-1)J_o\zeta_i + \mu_B H_o\right]\right\} \tag{11a}$$

$$\zeta_i = B_J\left\{\frac{1}{k_BT}\left[J(g-1)J_o\zeta_e + gJ\mu_B H_o\right]\right\} \tag{11b}$$

One should note that equations (11) correspond to two localized systems interacting via molecular fields (since $\tanh(x) = B_{1/2}(x)$). Although we have started with an itinerant - localized system, in the narrow-band limit we arrived at a result equivalent to two localized spins.

In the limit $T = T_c$ we have

$$\frac{1}{2}\left[\frac{k_B\theta'}{k_BT_c} + \frac{J(J+1)\ (g-1)^2}{3}\left(\frac{J_o}{k_BT_c}\right)^2\right] = 1 \tag{12}$$

From this equation one draws the equi-T_c curves (parabolae) in the plane $J(g-1)J_o \times k_B\theta'$ (Fig. 1), for k_BT_c=0.040eV, 0.062eV and 0.080 eV in the narrow - band limit. Figure 2 shows the electronic and ionic magnetizations ζ_e and ζ_i (from Eq. 11) and the corresponding inverse susceptibilities for pairs of parameters $(k_B\theta'; J(g-1)J_o)$ for the same values of T_c. It is worth noting that the curves of ζ_i versus T (for J=7/2) are more sensitive to changes in parameters $k_B\theta'$ and $J(g-1)J_o$ than the corresponding curves $\zeta_e(T)$. The inverse susceptibilities may show deviations from the Curie-Weiss law (Fig. 2a and 2b). Note in Fig. 2c and 2d that the paramagnetic Curie temperatures of the ionic and electronic magnetizations are near zero and T_c, respectively. In the extreme situation depicted in Fig. 2d, $J(g-1)J_o \simeq k_B\theta'/80$, the magnetism is sustained practically only by the intra-band interaction, and the ions, although having the same T_c of the band, exhibit a nearly paramagnetic response. Note that $\zeta_i(T)$ is nowhere larger than $\zeta_e(T)$, for a given T_c. In Fig. 2b, for intermediate temperatures, the curvature of ζ_e is smaller than that of ζ_i (see Section 5).

4. WIDE BAND (PARABOLIC DENSITY OF STATES)

In this case equations (4a) and (4b) are written

$$\int_0^\infty \frac{n(\varepsilon)d\varepsilon}{e^{\beta(\varepsilon-\mu_B H_e-\mu)}+1} - \int_0^\infty \frac{n(\varepsilon)d\varepsilon}{e^{\beta(\varepsilon+\mu_B H_e-\mu)}+1} = N_e\zeta_e \qquad (13a)$$

$$\int_0^\infty \frac{n(\varepsilon)d\varepsilon}{e^{\beta(\varepsilon-\mu_B H_e-\mu)}+1} + \int_0^\infty \frac{n(\varepsilon)d\varepsilon}{e^{\beta(\varepsilon+\mu_B H_e-\mu)}+1} = N_e \qquad (13b)$$

where $n(\varepsilon) = \frac{3}{4} N_e \frac{\varepsilon^{1/2}}{\varepsilon_o^{3/2}}$ and ε_o is the free electron Fermi energy,

$$\int_0^{\varepsilon_o} n(\varepsilon)d\varepsilon = N_e/2 \qquad (14)$$

Using the expression for H_e and H_i from Section 2, equations 13 can be re-written

$$F(\eta+\gamma) - F(\eta-\gamma) = \frac{4}{3}\left(\frac{\varepsilon_o}{k_B T}\right)^{3/2} \zeta_e \qquad (15a)$$

$$F(\eta+\gamma) + F(\eta-\gamma) = \frac{4}{3}\left(\frac{\varepsilon_o}{k_B T}\right)^{3/2} \qquad (15b)$$

where

$$\eta = \mu / k_B T \tag{16a}$$

$$\gamma = \left(\frac{k_B\theta'}{\varepsilon_o}\right)\left(\frac{\varepsilon_o}{k_B T}\right)\zeta_e + J\,(g-1)\left(\frac{J_o}{\varepsilon_o}\right)\left(\frac{\varepsilon_o}{k_B T}\right)\zeta_i + \left(\frac{\mu_B H}{\varepsilon_o}\right)\left(\frac{\varepsilon_o}{k_B T}\right) \tag{16b}$$

and

$$F(\alpha) = \int_0^\infty \frac{x^{1/2}}{e^{x-\alpha}+1}\, dx \tag{16c}$$

In the limit T=0 equations (15) and equation (4c) lead to

$$(1+\zeta_e)^{2/3} - (1-\zeta_e)^{2/3} = 2\left(\frac{k_B\theta'}{\varepsilon_o}\right)\zeta_e + 2J(g-1)\left(\frac{J_o}{\varepsilon_o}\right) \tag{17}$$

In the plane $J(g-1)J_o/\varepsilon_o$ x $k_B\theta'/\varepsilon_o$ the equi-$\zeta_e(0)$ curves are straight lines (Eq. 17). These are shown in Fig. 3 for $\zeta_e(0)=$ = 0.23, 0.26 and 0.50. These straight lines cut the axis $k_B\theta'/\varepsilon_o$ near 2/3, which is the minimum value of $k_B\theta'/\varepsilon_o$ for Stoner-type magnetic order.

In the limit $T=T_c$, one can obtain from (15) and (4c)

$$F'(\eta_c) = \frac{2}{J(J+1)(g-1)^2 \dfrac{(J_o/\varepsilon_o)^2}{k_B T_c/\varepsilon_o} + \dfrac{3k_B\theta'}{\varepsilon_o}} \; \frac{1}{\left(\dfrac{k_B T_c}{\varepsilon_o}\right)^{1/2}} \tag{18a}$$

$$F(\eta_c) = \frac{2}{3}\,\frac{1}{\left(\dfrac{k_B T_c}{\varepsilon_o}\right)^{3/2}} \tag{18b}$$

In Fig. 4, equi-T_c curves are shown in the plane $J(g-1)J_o/\varepsilon_o$ x $k_B\theta'/\varepsilon_o$. To draw these curves we have made use of the expression (Mc Dougall and Stoner (1938))

$$F(\alpha) \simeq \frac{2}{3} \alpha^{3/2} (1+ \frac{\pi^2}{8} \alpha^{-2}) \qquad (19)$$

valid for $\alpha >> 1$.

Figure 5 shows the electronic and ionic magnetizations and inverse susceptibilities, for increasing values of $k_B\theta'/\varepsilon_o$, fixing $k_BT_c/\varepsilon_o = 0.0155$.

The values of $k_B\theta'/\varepsilon_o$ were chosen in correspondence with those adopted in the study of the narrow band case (Section 3). It can be observed that the electronic magnetizations and inverse susceptibilities are more sensitive to the variations in $k_B\theta'/\varepsilon_o$ than the ionic quantities.

5. COMPARISON WITH EXPERIMENTAL DATA

The intermetallic compounds formed with the rare-earth metals and d-transition metals correspond to metallic systems where localized (4f) magnetic moments coexist with (s,d) itinerant moments. In the RM_2 compounds, for instance, one finds several magnetic "types" (Gomes and Guimarães (1974)): a) systems like YCo_2, where $T_c \simeq 0K$; b) systems where the intra-band interaction is responsible for the magnetic order (e.g. YFe_2); c) systems where the intra-band interaction is smaller, and the magnetism is driven by the 4f moments (e.g. $GdNi_2$) and finally, d) systems where 4f moments and d-d interactions are important, like $GdFe_2$.

In the framework of the present model we have studied how the critical temperature T_c depends on a) the rare-earth de Gennes factor in the RAl_2 and RFe_2 compounds (Fig. 6) and on b) the relative concentrations of the transition metal in sys tems like $R(Al_{1-x}Fe_x)_2$, where the ratio of the number of rare - earth atoms to transition metal atoms varies along the series. In this study we have taken $J_o = 2.1 \times 10^{-3}$eV independently of x and independently of which heavy rare-earth is present. For the compound RAl_2 (x=0) we have taken ε_o = 8eV and $k_B\theta'/\varepsilon_o$ slightly below 2/3, whereas for x=1 (RFe_2), ε_o = 4 eV and $k_B\theta'/\varepsilon_o$ is slightly above 2/3. The choice of the ε_o's corresponds to the fact that the transition metal has a narrower band; the parameter $k_B\theta'/\varepsilon_o$ was chosen taking into account that YAl_2 is non-magnetic ($k_B\theta'/\varepsilon_o \leq 2/3$) and that YFe_2 is magnetic ($k_B\theta'/\varepsilon_o > 2/3$).

The curve of T_c (or T_N) versus rare-earth de Gennes factor computed for the compounds RAl_2, with $k_B\theta'/\varepsilon_o$ slightly below 2/3 and $J_o = 2.1 \times 10^{-3}$ eV is shown in Fig. 6a. We have imposed that T_c (YAl_2) = 0K and $T_c(GdAl_2)$ = 200K. The same curve for the RFe_2 compounds was computed with $k_B\theta'/\varepsilon_o$ slightly above 2/3 and again $J_o = 2.1 \times 10^{-3}$ eV (Fig. 6b). The end-points are $T_c(YFe_2)$ = = 542K and T_c ($GdFe_2$) = 796K. The first curve (for the RAl_2 compounds) is a straight line, and the second (RFe_2) is almost straight, with a slight curvature; this agrees with the general linear dependence observed experimentally (Taylor (1971)).

For $0 \leq x \leq 1$ in the $Gd(Al_{1-x}Fe_x)_2$ we have assumed, for simplicity, a linear dependence of $k_B\theta'/\varepsilon_o$ on x:

$$\left(\frac{k_B\theta'}{\varepsilon_o}\right)_{Gd(Al_{1-x}Fe_x)_2} = \left(\frac{k_B\theta'}{\varepsilon_o}\right)_{GdAl_2} + x\left[\left(\frac{k_B\theta'}{\varepsilon_o}\right)_{GdFe_2} - \left(\frac{k_B\theta'}{\varepsilon_o}\right)_{GdAl_2}\right] \qquad (20)$$

The computed Curie temperatures versus x are shown in Fig. 7, for two band widths (ε_o = 4eV and 8eV), and $J_o = 2.1 \times 10^{-3}$eV; Fig. 7 also shows that $T_c(x)$ is not too sensitive to such varia tio in ε_o.

It is interesting to observe that we have been able to compute the curves of Fig. 6 and Fig. 7 using the same value of J_o (and of the right order of magnitude). This imposes a non-vanishing value for $k\theta'/\varepsilon_o$ (slightly below 2/3) in the case of RAl_2, suggesting that intraband exchange enhancement effects may be relevant in this series.

It is worth noting that the computed electronic and ionic magnetizations M_e and M_i, in the narrow-band limit (Fig.2) show some distinctive qualitative features observed in published experimental results. In Fig. 2a the ionic magnetization tends to show less curvature than the electronic magnetization, for intermediate temperatures. This effect is present in the measured total magnetization M($M = M_i + M_e$), e.g., of Gd-Fe intermetallic compounds; the magnetization of Gd_2Fe_{17} (where the electronic, i.e., 3d magnetization, is dominant) is more convex, whereas for $GdFe_2$, with a relatively larger contribution of M_i, M is almost straight in the middle range of T (Fig. 10 in Burzo (1980)). The same trend is found when we compare ^{57}Fe hf fields (which are grossly proportional to M_e) to the rare-earth hf fields (roughly αM_i) in R_xFe_y intermetallic compounds (e.g., in $DyFe_2$ (Bowden et al. (1968)).

The present model, although simple, allows the computation of magnetic quantities ($\zeta(T)$, $\chi(T)$ and T_c) that behave in a similar way to the numbers obtained experimentally. In our presentation we have emphasized the combined role of intraband and electron-ion coupling parameters in determining the temperature dependence of the magnetizations and susceptibilities .

A deeper analysis, with vista to fit the experimental values of the available magnetic data, should consider, eventually increasing the degree of complexity: a more realistic band description (taking into account degeneracy and s-d mixture), adequate g factors for the electronic magnetization and proper consideration for crystal field effects.

ACKNOWLEDGEMENTS

L.I. acknowledges a research fellowship from CNPq/Brasil.

REFERENCES

Bloch D, Edwards D M, Shimizu M and Voiron J 1975 J. Physics F: Metal Phys. 5 1217-1226.

Bloch D and Lemaire R 1970 Phys. Rev. B2 2648-2650.

Borgiel W, Kozarzewski B and Witanski K 1980 Acta Phys. Pol. A58 529-534

Bowden G J, Bunbury D St P, Guimarães A P and Snyder R E 1968 J. Phys. C 1 1376-1387.

Burzo E Vth School on Theoretical Physics, Silesian University, September 1980, lecture notes.

Buschow K H J 1977 Repts. Progr. Phys. 40 1179-1256.

Debray D and Sakurai J 1974 Phys. Rev. B9 2129-2133.

Gomes A A and Guimarães A P 1974 J. Phys. F: Metal Phys. 4 1454-1465.

Herring C in Magnetism vol. IV, Rado G T and Suhl H ed, Academic Press, 1966.

Ilarraz J and del Moral A 1980 Phys. Stat. Sol. 57a 89-98.

Kirchmayr H R and Poldy C A 1978 J. Magn. Magn. Mater. 8 1-42.

Mc Dougall J and Stoner E C 1938 Phil. Trans. Roy. Soc. 237 67-104.

Sakoh M and Edwards D M 1975 Phys. Stat. Sol. 70b 611-618.

Stearns M B 1973 Phys. Rev. B8 4383-4398.

Stoner E C 1951 J. Phys. Radium 12 372-388.

Taylor K N R 1971 Adv. Phys. 20 551-660.

Wohlfarth E P 1979 J. Phys. F: Metal Phys. 9 L123-128.

FIGURE CAPTIONS

Fig. 1 - Equi-T_c curves (parabolae) in the plane $J(g-1)J_o$ x $k_B\theta'$ for k_BT_c = 0.04eV, 0.062eV and 0.080eV, in the narrow band limit for J = 7/2.

Fig. 2 - Ionic (i) and electronic (e) magnetizations and inverse susceptibilities versus temperature in the narrow band limit for pairs ($J(g-1)J_o$; $k_B\theta'$): a) $k_B\theta'$ = 0eV, $J(g-1)J_o$= = 0.134 eV; b) 0.08eV and 0.08eV; c) 0.123eV and 0.0125eV; d) 0.124eV and 0.001614eV, for k_BT_c = 0.0620eV.

Fig. 3 - Equi-$\zeta_e(0)$ (eletronic magnetizations at T=0) curves (straight lines) in the plane $J(g-1)J_o/\varepsilon_o$ x $k_B\theta'/\varepsilon_o$ for the following values of $\zeta_e(0)$: 0.23, 0.26 and 0.50 (the numbers are those of the electronic magnetizations of Fig. 5 for T=0).

Fig. 4 - Equi-T_c curves (parabolae) in the plane $J(g-1)J_o/\varepsilon_o$ x $k_B\theta'/\varepsilon_o$ for k_BT_c/ε_o = $0.04/\varepsilon_o$, $0.0620/\varepsilon_o$, $0.08/\varepsilon_o$ (taking ε_o = 4eV).

Fig. 5 - Ionic (i) and electronic (e) magnetizations and inverse susceptibilities versus temperature for k_BT_c/ε_o=$0.0620/\varepsilon_o$ and a) $k_B\theta'/\varepsilon_o$ = 0, $J(g-1)J_o/\varepsilon_o$ = 0.155, b) 0.1382 , 0.1382, c) 0.55, 0.065.

Fig. 6 - Calculated Curie temperatures versus rare-earth (R) de Gennes factors to simulate the RAl_2 and RFe_2 compounds a) for $k_B\theta'/\varepsilon_o$ = 0.6665, ε_o = 8eV; b) for $k_B\theta'/\varepsilon_o$ = = 0.6667, ε_o = 4eV. In both curves J_o = 2.1 x 10^{-3}eV . We have fixed the end-points at the values of T_c (or T_N) determined experimentally (see text).

Fig. 7 - Calculated Curie temperatures versus iron concentration (x) to simulate the $Gd(Fe_xAl_{1-x})_2$ system, for two band widths a) $\varepsilon_o = 4eV$ and b) $\varepsilon_o = 8eV$. Here, as in Fig.6, $J_o = 2.1 \times 10^{-3}eV$ and the end-points have been taken from the literature.

Fig 1 - L. Iannone et all

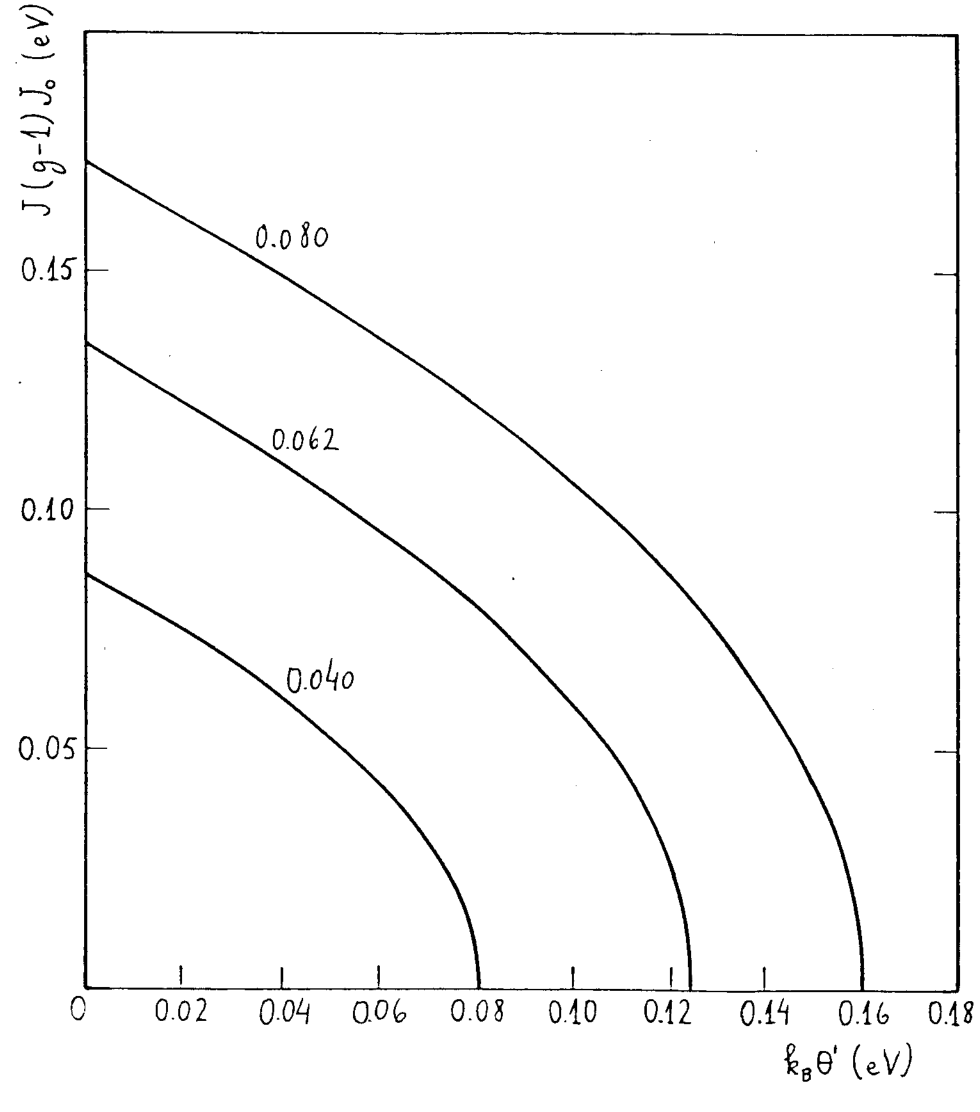

Fig 2a

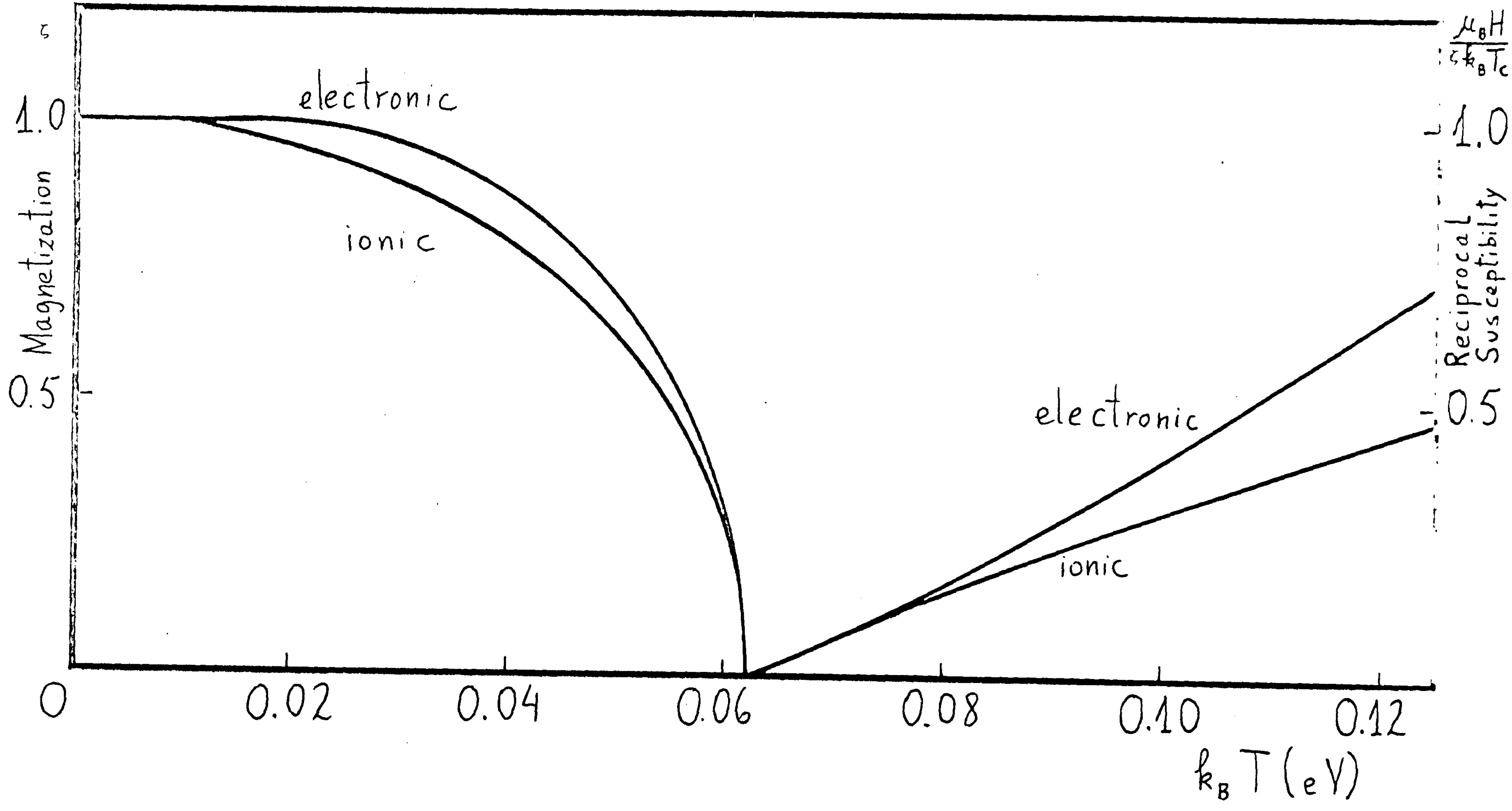

Magnetization
1.0
0.5
electronic
ionic
electronic
ionic
$\frac{\mu_B H}{5 k_B T_c}$
Reciprocal Susceptibility
1.0
0.5
0
0.02
0.04
0.06
0.08
0.10
0.12
$k_B T$ (eV)

Fig. 2b

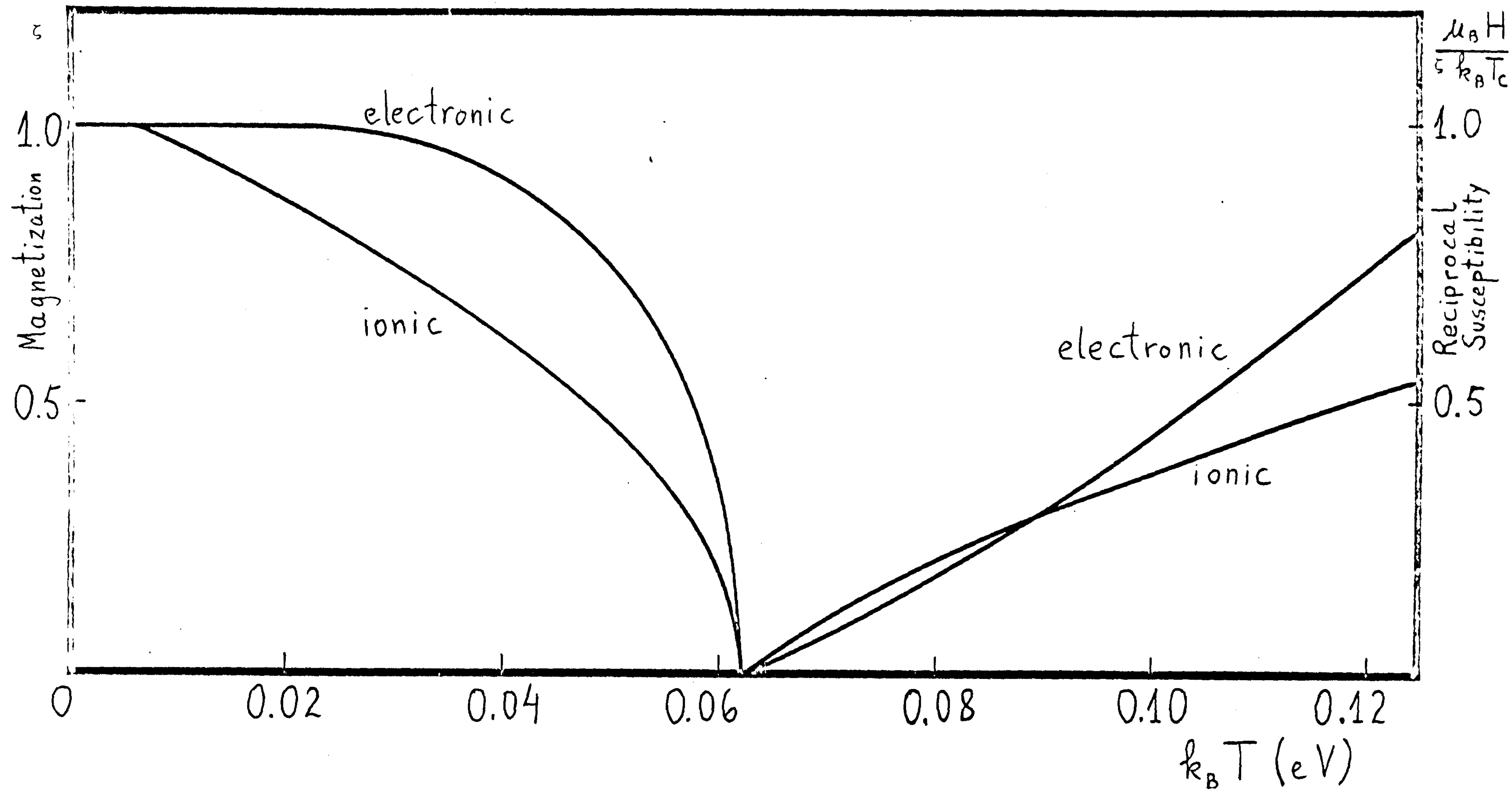

ζ
Magnetization
1.0
0.5
electronic
ionic
electronic
ionic
$\frac{\mu_B H}{\zeta k_B T_c}$
1.0
0.5
Reciprocal Susceptibility
0
0.02
0.04
0.06
0.08
0.10
0.12
$k_B T$ (eV)

Fig 2c

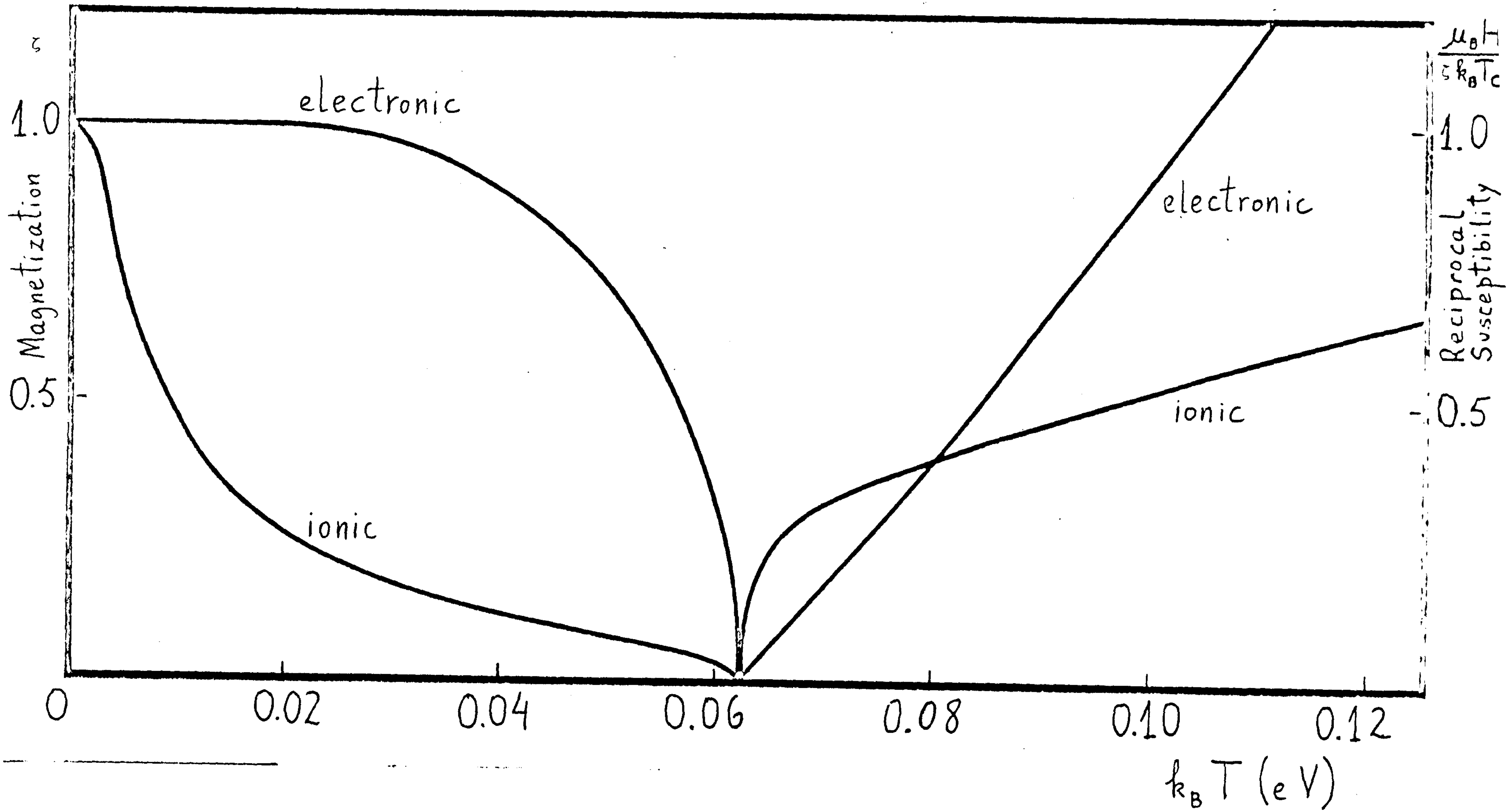

Magnetization
1.0
0.5
0
electronic
ionic
0.02
0.04
0.06
0.08
0.10
0.12
$k_B T$ (eV)
$\frac{\mu_B H}{\varsigma k_B T_c}$
Reciprocal Susceptibility
electronic
ionic
1.0
0.5

Fig 2d

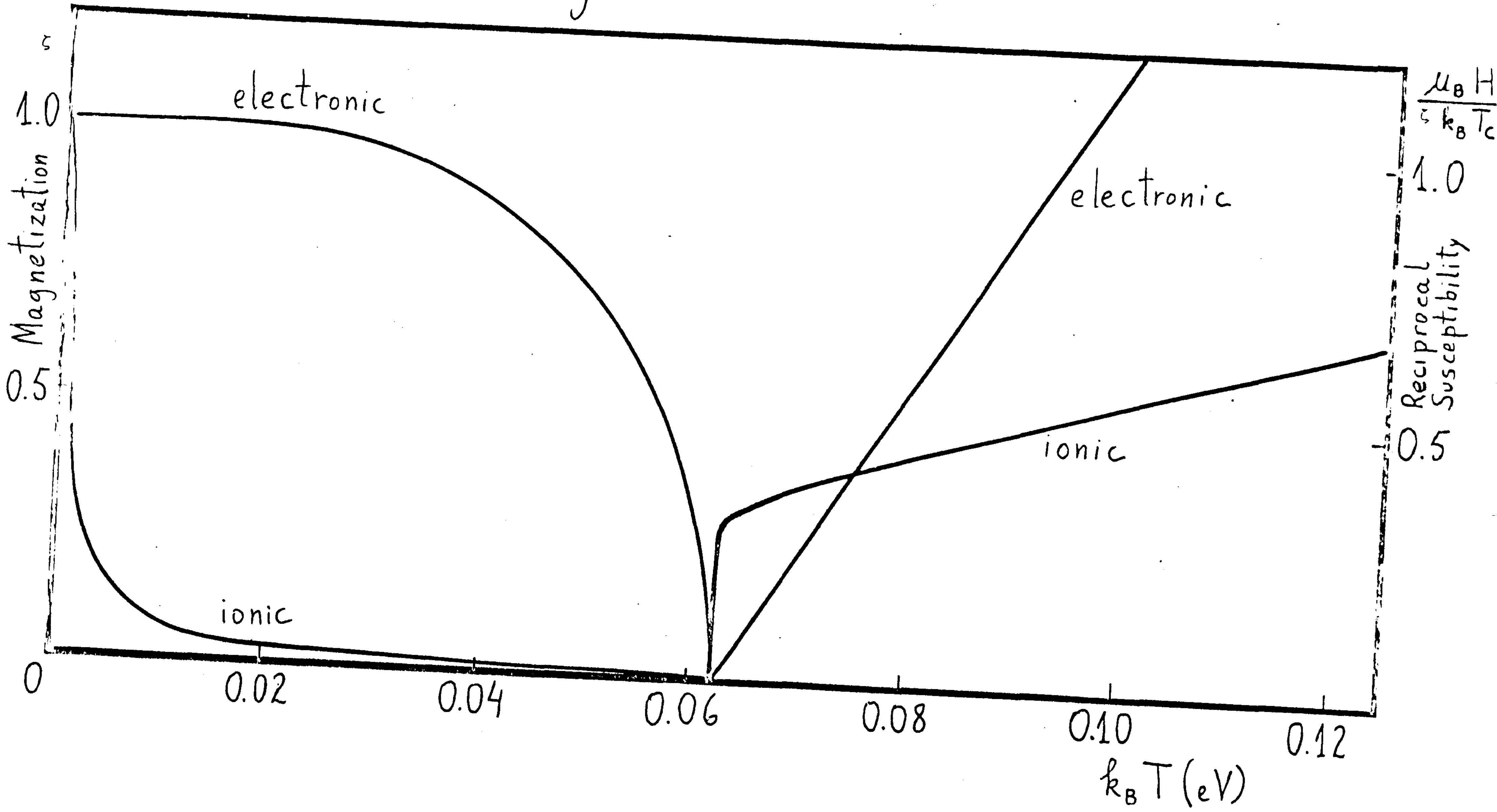

Magnetization
1.0
0.5
0
electronic
ionic
electronic
ionic
0.02
0.04
0.06
0.08
0.10
0.12
$k_B T$ (eV)
Reciprocal Susceptibility
$\frac{\mu_B H}{\varsigma k_B T_c}$
1.0
0.5

Fig. 3 L. Iannarella et al.

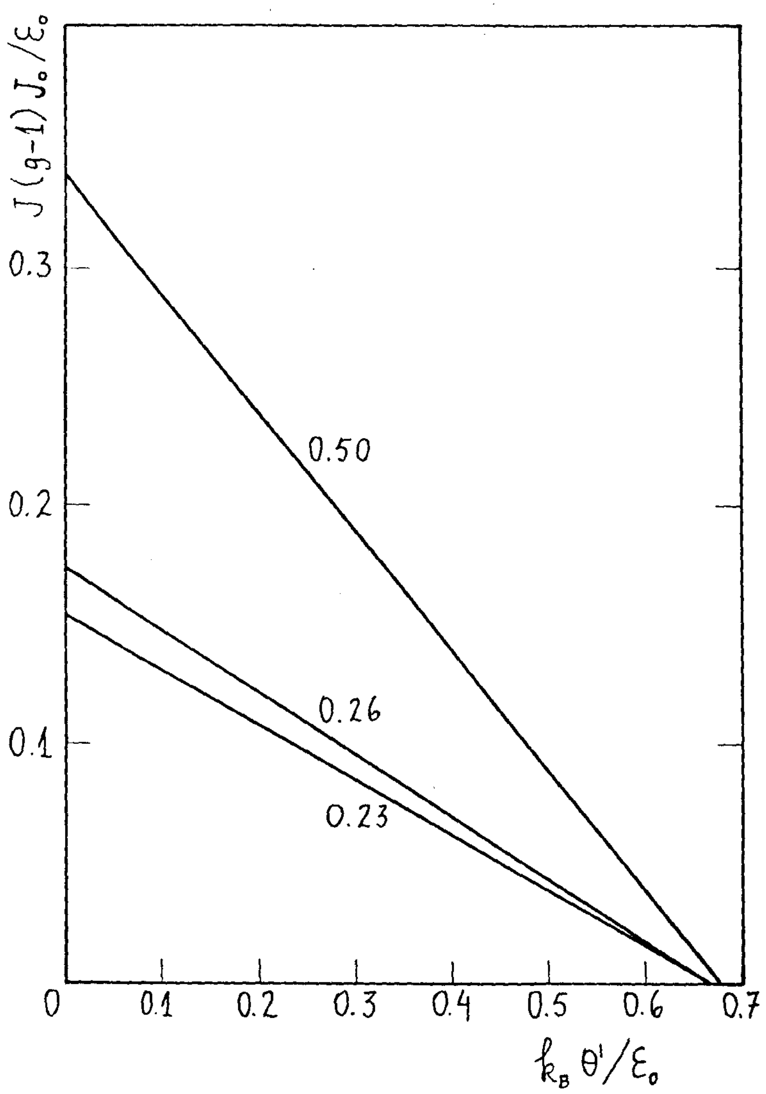

Fig. 4 L. Iannarella et al.

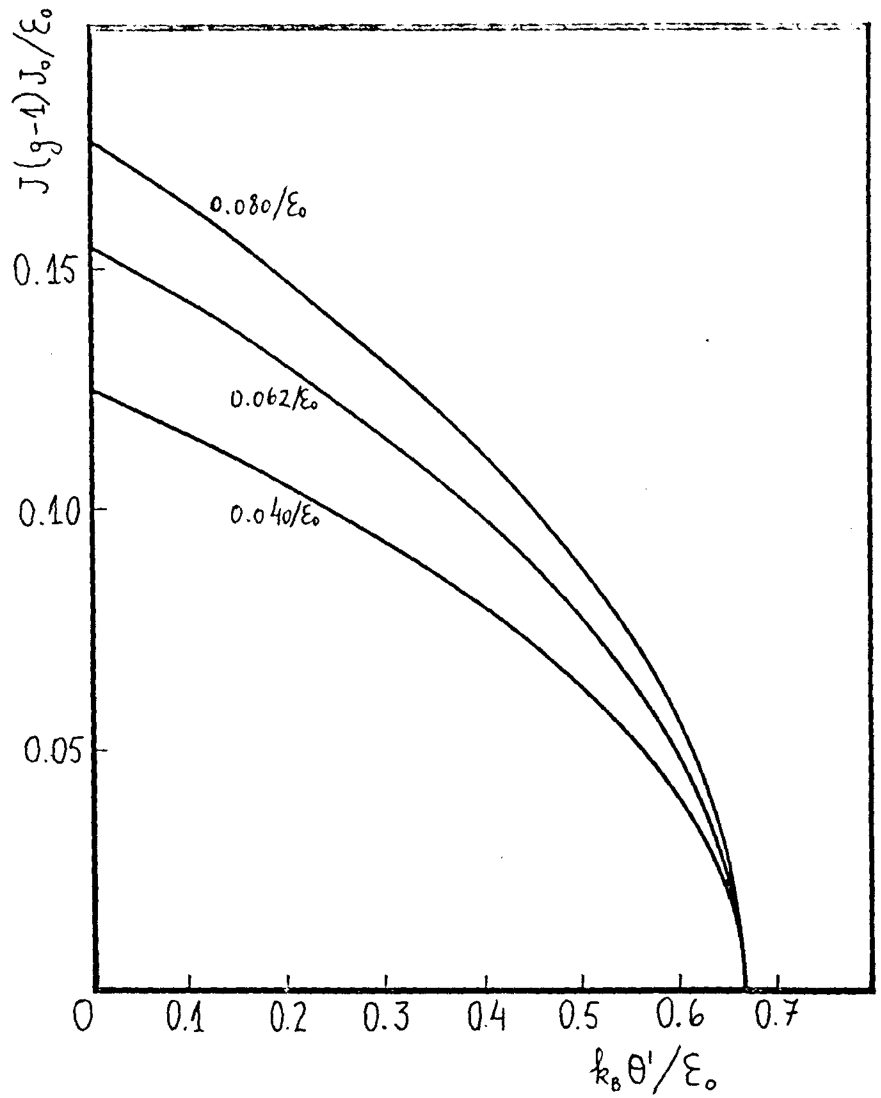

Fig. 5a

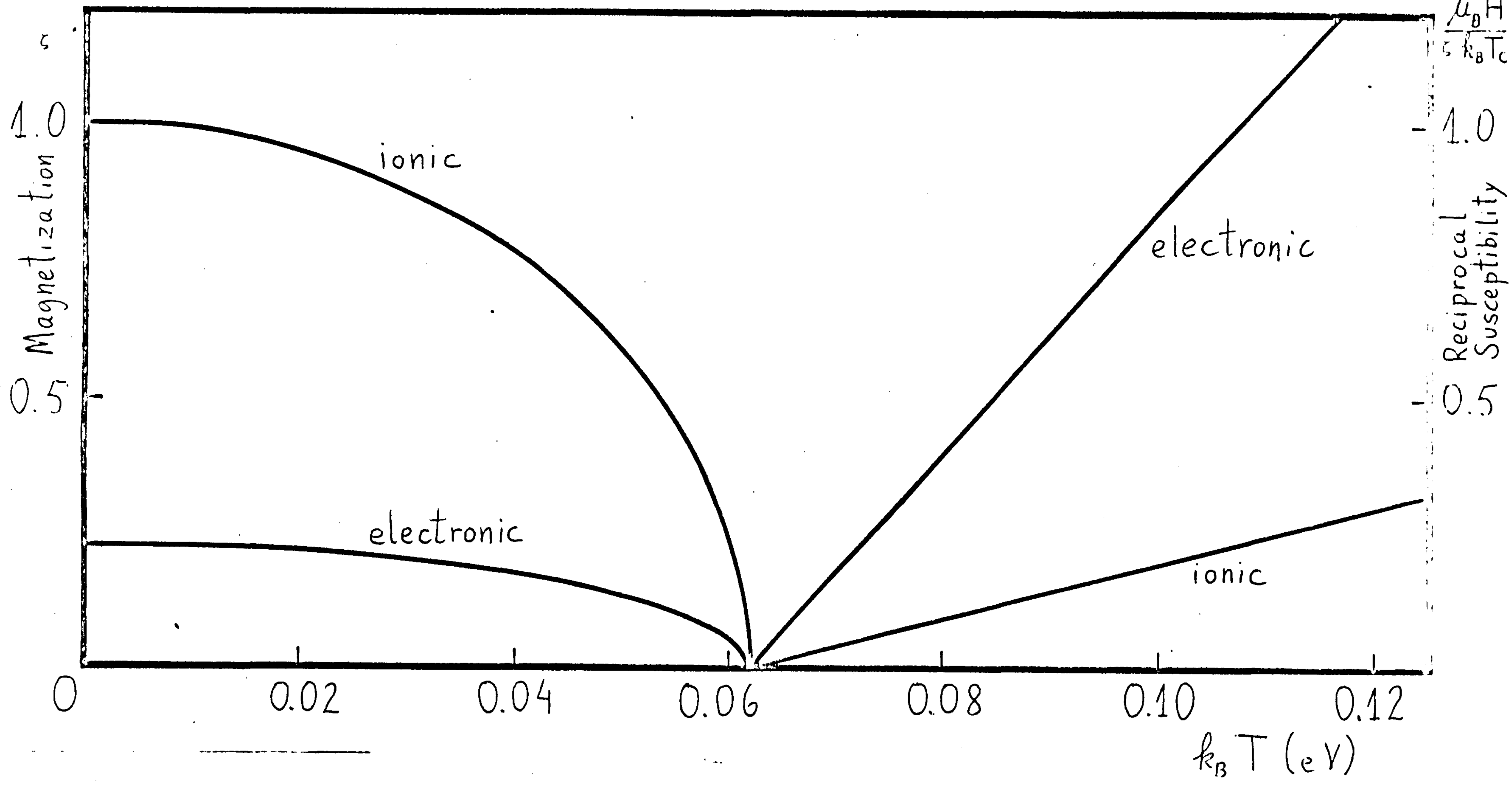

Magnetization
1.0
0.5
0
0.02
0.04
0.06
0.08
0.10
0.12
$k_B T$ (eV)
ionic
electronic
electronic
ionic
Reciprocal Susceptibility
$\frac{\mu_B H}{\varsigma k_B T_c}$
1.0
0.5

Fig. 5b

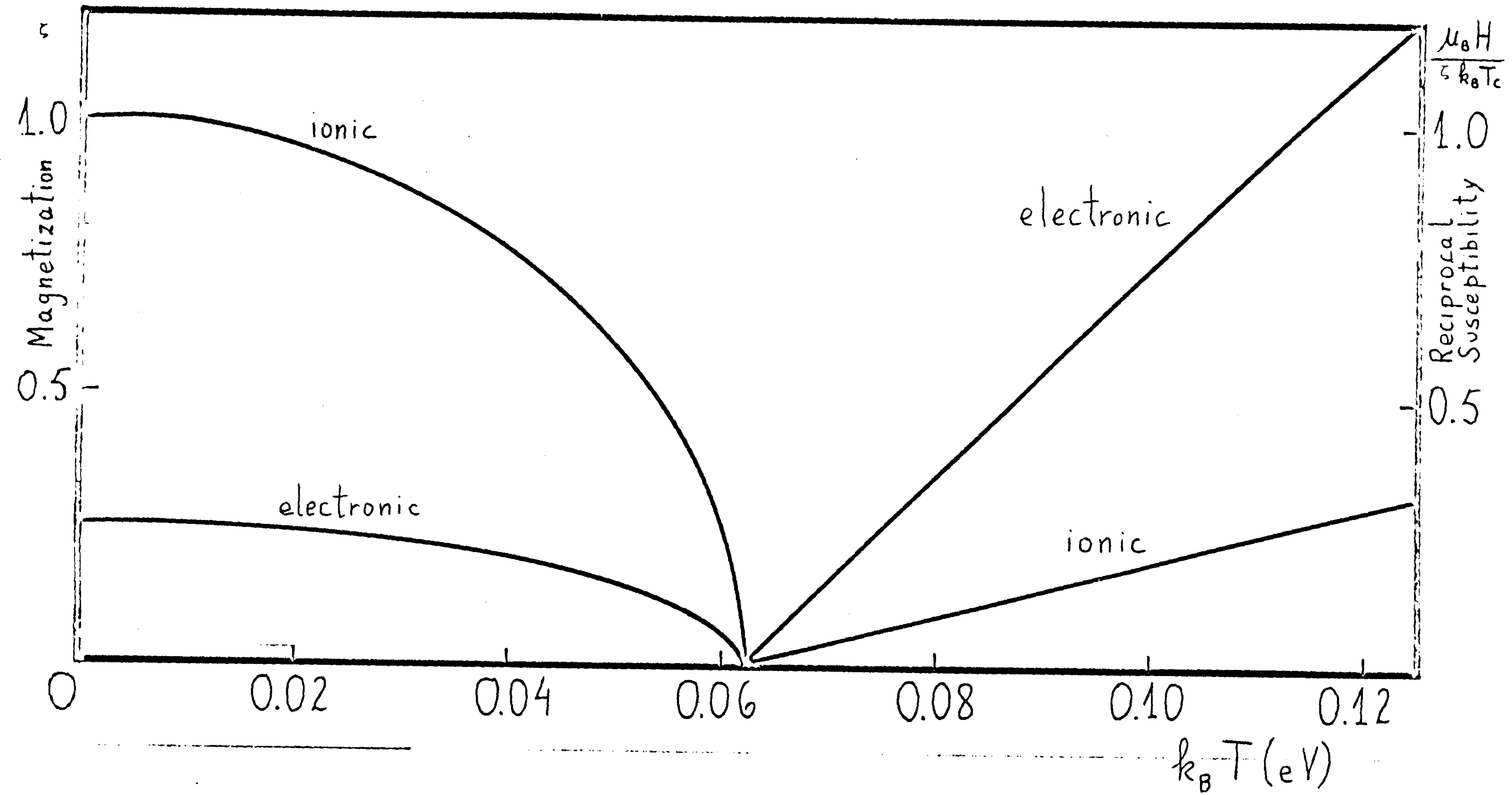

Magnetization
1.0
0.5
ionic
electronic
electronic
ionic
$\frac{\mu_B H}{\varsigma k_B T_c}$
Reciprocal Susceptibility
1.0
0.5
0
0.02
0.04
0.06
0.08
0.10
0.12
$k_B T$ (eV)

Fig. 5c

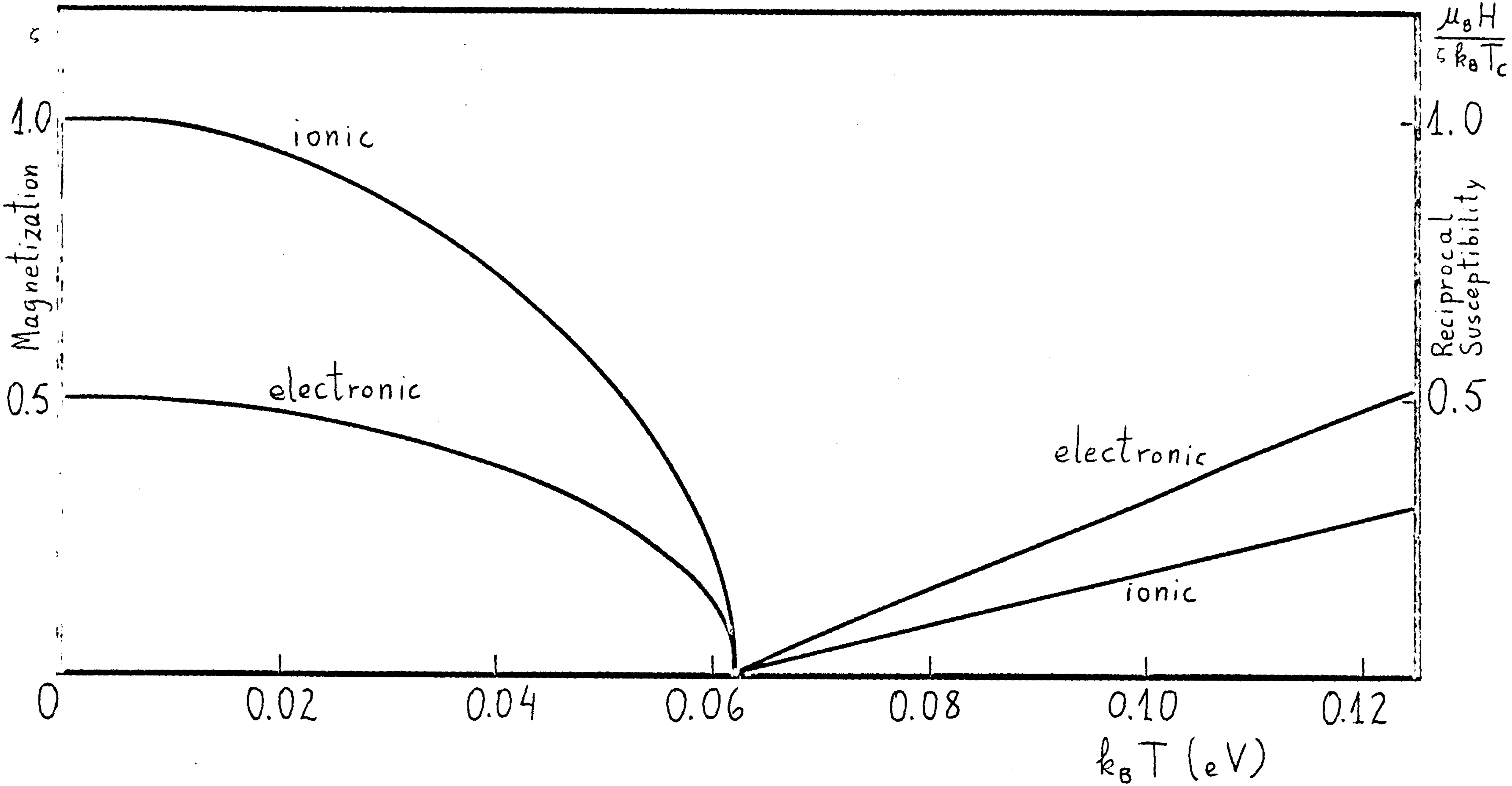

ς
1.0
0.5
Magnetization
ionic
electronic
electronic
ionic
0
0.02
0.04
0.06
0.08
0.10
0.12
$k_B T$ (eV)
$\frac{\mu_B H}{\varsigma k_B T_c}$
1.0
0.5
Reciprocal Susceptibility

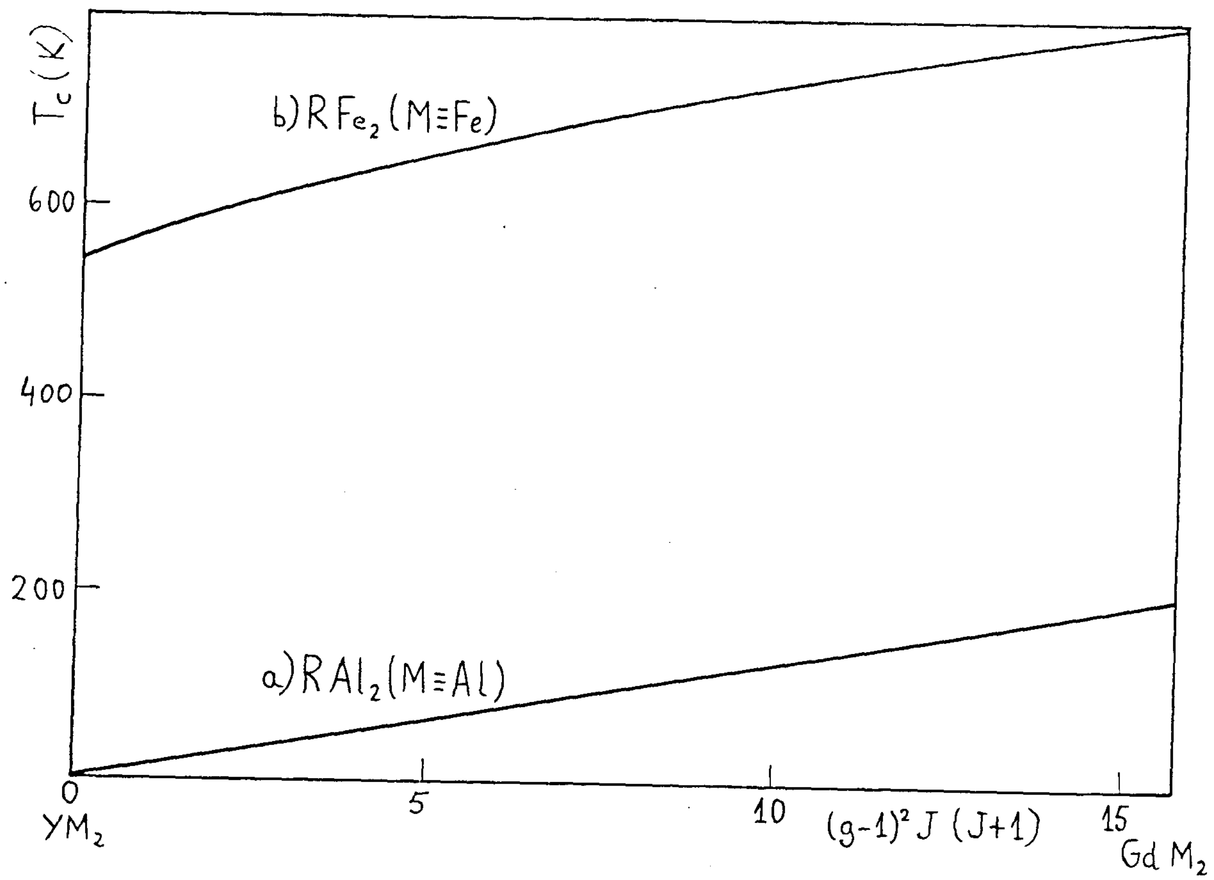
Tc (K)
600
400
200
b) RFe2 (M≡Fe)
a) RAl2 (M≡Al)
0
5
10
15
YM2
(g-1)² J (J+1)
Gd M2

Fig 7

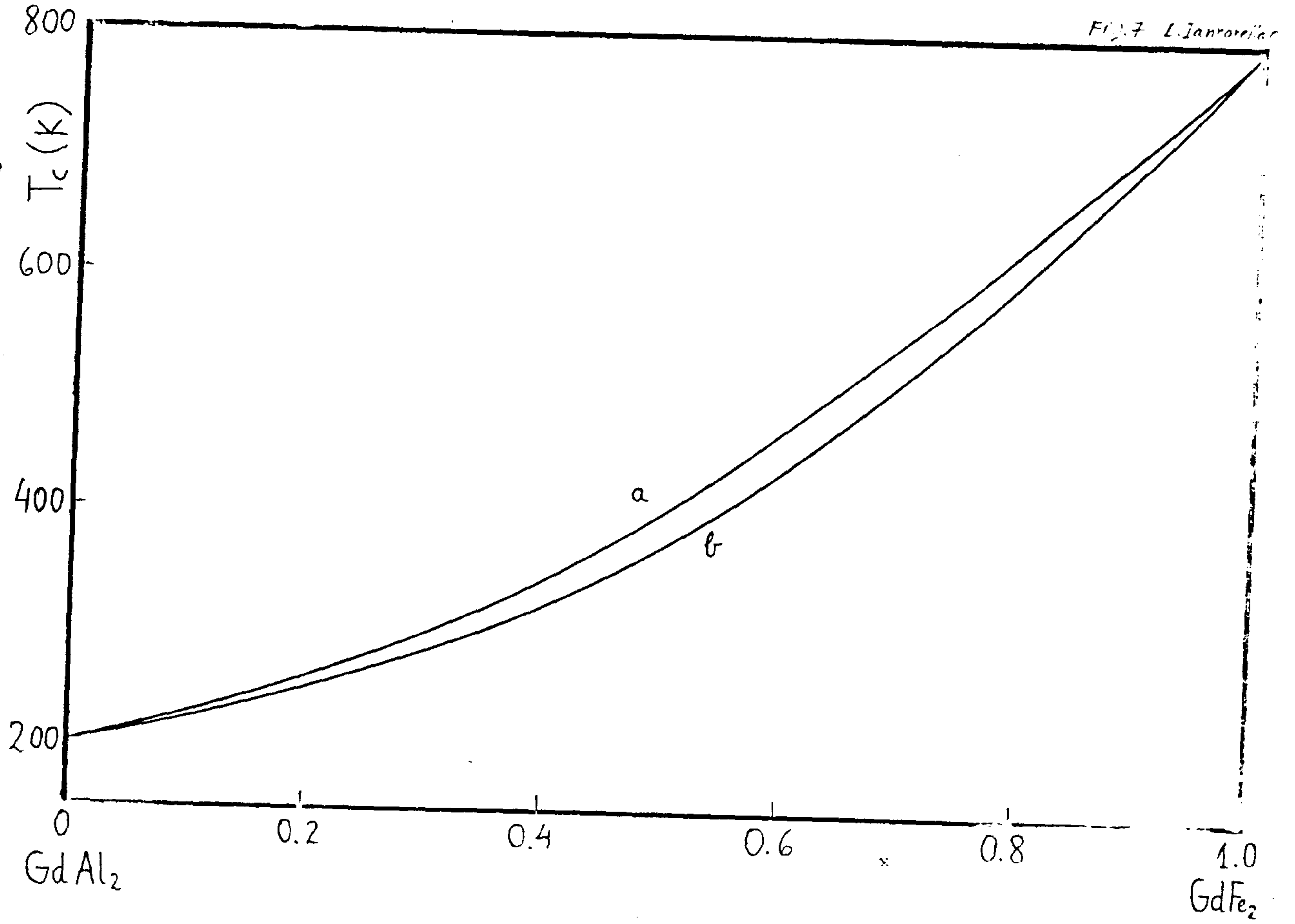
Fig.7 L.Iannarella
800
Tc (K)
600
400
200
a
b
0
0.2
0.4
0.6
0.8
1.0
Gd Al2
GdFe2